NASA Contractor Report 203877

Spectral and Spectral–Element Methods: Lecture Notes in High Performance Computational Physics

Anil E. Deane

GRANT NAG5–2652
JUNE 1997

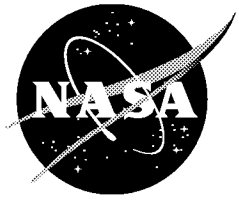

NASA Contractor Report 203877

Spectral and Spectral–Element Methods: Lecture Notes in High Performance Computational Physics

Anil E. Deane
George Mason University
Fairfax, VA 22030-4444

Prepared for
Goddard Space Flight Center
under Grant NAG5–2652

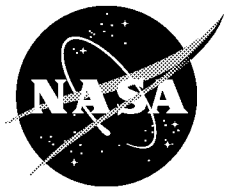

National Aeronautics
and Space Administration

Goddard Space Flight Center
Greenbelt, Maryland

1997

Spectral and Spectral-Element Methods: Lecture Notes in High Performance Computational Physics

Anil E. Deane
Institute for Computational Science and Informatics
George Mason University &
High Performance Computing Branch, MC 934,
Building 28, S213
NASA Goddard Space Flight Center
deane@laplace.gsfc.nasa.gov

Abstract

This is an introduction to spectral and spectral-element methods for the numerical simulation of incompressible and compressible hydrodynamics. The theory behind the methods is presented as well as some examples of working codes. The work is reasonably self-contained in that there is included a discussion of numerical quadrature, weighted residual methods, Fast Fourier Transforms and time marching schemes. The work is based on a set of lectures by the author for the NASA Summer School for High Performance Computational Physics, held at Goddard Space Flight Center.

Contents

List of Figures

List of Tables

1 SPECTRAL METHODS

1.1 Introduction

These lecture notes evolved from slides presented as part of some lectures on spectral and spectral-element methods to gradute students attending the NASA Goddard Space Flight Center's Summer School in High Performance Computational Physics. They should give the reader a very introductory feel for the subject. Far from being exhaustive they are incomplete even as a robust introduction. Nevertheless the material presented here is, to this author's knowledge, not available in a single place, being spread over various books and articles. A reading guide to the these is included at the end.

The lectures as presented in the summer school also included many results from large-scale simulations based on spectral and spectral-element methods illustrating the power and practice of these methods. These have not been included in this set of lecture notes. Also not included is a discussion of parallelization issues. These omissions will, it is hoped, become remedied at a later date in a revised version.

The Fourier basis is the most commonly encountered basis set of orthogonal expansion functions. In later sections, when we talk of other basis functions, such as Chebyshev and Legendre functions, the Fourier basis will guide our intuition. The reader is presumably familiar with the wide scope of application that they have enjoyed in the physical sciences. In these lectures we are concerned with the solution of partial differential equations by spectral methods, particularly those equations that arise in fluid dynamics.

At first it may not be apparent why Fourier basis are at all relevant in fluid dynamics problems. We are familiar with the phenomenon of turbulence. This much studied problem is often discussed using the jargon "power spectrum", "wavenumber","wavenumber space", "triad interactions", "pdf" (probability distribution function) etc. In fact these terms refer to the representation of the flow in the Fourier basis. How is it though that a basis set that is periodic in nature can be such an important tool in the representation of the (spatial) flow when there are boundaries present? Certainly *homogeneous* turbulence can be so represented, but most flows are *not* homogeneous, since they possess boundaries. The reason why the Fourier basis and homogeneous turbulence continues to be important is because at high

Reynolds numbers, the flow away from the boundaries does not "feel" the presence of the boundaries. Thus small regions of within the domain contain enough range of scales so as to treatable as periodic without too much error. Naturally when dealing with the flow near boundaries, an expansion in another, non-periodic basis becomes necessary.

In numerical analysis one encounters the Fourier basis again. In the Von-Neumann stability analysis (see Chapter 3) it is convenient to talk of different wavenumbers being damped. This convenience arises because of Fourier's theorm. Again, when looking at the behavior of schemes with boundary conditions involved such convenience must be dropped for stability analysis based on matrices.

1.2 Spectral Methods for Solution of PDEs

For smooth flow — flows that do not have shocks or sharp fronts, spectral methods provide high accuracy and exponential convergence to the soulution.

Consider Table 1.2 where a comparision is made between a Fourier method and finite differences.

N	Fourier-Galerkin	2FD	4FD
8	9.87×10^{-2}	1.11	9.62×10−1
16	2.55×10^{-4}	6.13×10−1	2.36×10−1
32	1.05×10^{-11}	1.99×10−1	2.67×10−2
64	6.22×10^{-13}	5.42×10−2	1.85×10−3
128	-	1.37×10−2	1.18×10−4

Table 1: Error in the solution of $\frac{\partial u}{\partial t} = \frac{\partial u}{\partial x}$. Reproduced from Canuto et al.

For a fixed error, determined by how accurately one wants the solution, say of the order of 10^{-4}, according to the table one needs a smaller number of grid points, N for spectral solution. Although the table is shown for Fourier method, the essential result is the sam for Chebyshev, Legendre or other basis (provided the basis chosen is suitable for the boundary conditions).

The conclusion to be drawn from this is that *any method which has these accuracy and convergence properties is obviously of interest.*

Many key problems have been solved using spectral techniques, in hydrody-

namic stability, transition and turbulence.

Table 2 summarizes these calculations and cites the key references.

Domain	Physics	Investigators
Box	homogeneous turbulence	Orszag
Box	sheared turbulence	Wray, Rogallo,Moin, Kim, Herring
Box	channel flow	Orszag, Patera, Moin, Kim
Box	Magnetohydrodynamics (MHD)	Orszag, Tang, Matthaues, Dahlburg
Box	convection	Orszag, Herring
semi-infinite	boundary layers	Spalart, Zang, Hussaini
cylinderical	Taylor-Couette	Streett, Marcus
semi-infinite	shear layer	Orszag, Riley, Metcalf
sphere	Earth core, mantle	Glatzmaier, Tackley

Table 2: Spectral methods applications

Three problems arise for spectral methods. Spectral methods are restricted to:

1. **Simple geometry.** Although variety of boundary conditions, and variable coefficients can be handled (well) the restriction to simple geometries is irksome. Solved by *domain decomposition* and *Spectral-Element methods.*

2. **Smooth flow.** Gibbs phenomena associated with the representation of discontinuities. Solved by *filters* and *spectral- FCT* methods.

3. **Parallelization.** Spectral transforms are communication intensive. Solved by *Spectral-element methods.*

1.3 Gaussian Quadrature

There is a unique N-th order polynomial through $N+1$ points, called the *interpolating polynomial.*

One could compute it via:

$$\sum_{k=0}^{N} a_k x_i^k = f(x_i) \qquad i = 0, 1, \ldots N,$$

provided the *Vandermonde determinant*, $|x_i^k| \neq 0$. But this is inefficient. Instead compute it via:

(a) Newton's divided differences

$$f(x) \approx p(x) = f(x_0) + (x - x_0) f[x_1, x_0] + (x - x_0)(x - x_1) f[x_2, x_1, x_0] + R(x)$$

where

$$f[x_1, x_0] = \frac{f(x_1) - f(x_0)}{x - x_0},$$

and

$$f[x_2, x_1, x_0] = \frac{f[x_2, x_1] - f[x_1, x_0]}{x_2 - x_0}$$

and

$$R(x) = (x - x_0)(x - x_1)(x - x_2) f[x, x_2, x_1, x_0]$$

is error term.

(b) Lagrange Interpolation

$$p_i(x) = \frac{(x - x_0)(x - x_1) \dots (x - x_{i-1})(x - x_{i+1}) \dots (x - x_N)}{(x_i - x_0)(x_i - x_1) \dots (x_i - x_{i-1})(x_i - x_{i+1}) \dots (x_i - x_N)} \quad i = 0, 1, \dots N$$

or

$$p_i(x) = \frac{\alpha(x)}{(x - x_i)\alpha'(x_i)}$$

$$P(x) = \sum_{i=0}^{N} p_i(x) f(x_i$$

Thus

$$P(x) = \sum_{i=0}^{N} \frac{\alpha(x)}{(x - x_i)\alpha'(x_i)} f(x_i)$$

is the Lagrange Interpolating Polynomial of degree N.

Note that $p_i(x_i) = 1$ and $P(x_i) = f(x_i)$

and $\alpha(x) = (x - x_0)(x - x_1) \ldots (x - x_N)$ is of degree $(N + 1)$.

Suppose we want to evaluate

$$\int_a^b f(x')w(x')dx'$$

where $w(x')$ is some "weight" function.

By the transformation

$$x' = \frac{b-a}{2}x + \frac{b+a}{2}$$

leads us to consider only:

$$\int_{-1}^{1} f(x)w(x)dx$$

Because of the availability of this transformation, from now on we need consider only the interval [-1,1].

Let this integral be

$$\int_{-1}^{1} f(x)w(x)dx = \sum_{i=0}^{N} a_i f(x_i)$$

where x_i are the points where $f(x)$ is evaluated, and a_i are some coefficients.

Number of unknowns is:

$N + 1$ a_i

$N + 1$ x_i

1 N itself

or $2N + 3$ unknowns. Let

$$f(x) = P(x) + r(x)$$

where $P(x)$ is an N-th degree polynomial.

If we take

$$P(x) = \sum_{i=0}^{N} \frac{\alpha(x)}{(x - x_i)\alpha'(x_i)} f(x_i)$$

Then

$$\int_{-1}^{1} f(x)w(x)dx \approx \int_{-1}^{1} P(x)w(x)dx$$

$$= \int_{-1}^{1} \sum_{i=0}^{N} f(x_i) \frac{\alpha(x)}{(x - x_i)\alpha'(x_i)} w(x)dx$$

$$= \sum_{i=0}^{N} f(x_i) \int_{-1}^{1} \frac{\alpha(x)}{(x - x_i)\alpha'(x_i)} w(x)dx$$

$$= \sum_{i=0}^{N} a_i f(x_i)$$

If we take $x_i = x_0 + i\Delta x$ (equally spaced points), we get the *Newton-Cotes* formulae (e.g. the familiar Simpson's rule). But if x_i are *not* equally spaced, then we obtain an important result:

Newton-Cotes formulae are exact (at $x = x_i$) for polynomials $f(x)$ of degree N. But if x_i are such that they are *Gauss points*, ie. zero's of the $(N + 1)$-th order polynomial $\alpha(x)$ constructed such that it is orthogonal to all lower degree polynomials makes the integration exact for $f(x)$ polynomial of degree up to $2N + 1$.

So

$$\int_{-1}^{1} \alpha(x)q(x)w(x) = 0$$

α orthogonal to $q(x) \in \mathcal{P}_{\leq N}$

Let

$$f(x) \in \mathcal{P}_{\leq 2N+1}$$

$$\frac{f(x)}{\alpha(x)} = q(x) + \frac{\rho(x)}{\alpha(x)}$$

Here $\rho(x)$ and $q(x)$ are $\mathcal{P}_{\leq N}$, while $\alpha(x)$ is $\mathcal{P}_{\leq N+1}$. This is a standard result known as the *Division Theorm* of polynomials.

This can be written

$$f(x) = \alpha(x)q(x) + \rho(x)$$

Integrating over interval

$$\int_{-1}^{1} f(x)w(x)dx = \int_{-1}^{1} \alpha(x)q(x)w(x)dx + \int_{-1}^{1} \rho(x)w(x)dx$$

The first term on the RHS drops out because of the assumed orthogonlity.

Since $\rho(x)$ is $\mathcal{P}_{\leq N}$

$$\int_{-1}^{1} \rho(x)w(x)dx = \sum_{i=0}^{N} a_i\rho(x_i)$$

is exact.

Now

$$f(x_i) = \alpha(x_i)q(x_i) + \rho(x_i)$$

the first term is zero because $\alpha(x_i) = 0$ leading to

$$\int_{-1}^{1} f(x)w(x)dx = \sum_{i=0}^{N} a_i f(x_i)$$

Hence by arranging our quadrature points we are able to represent polynomials of degree $2N+1$ *exactly*.

Now we make the identification

$$\alpha_{N+1}(x) \equiv L_{N+1}(x) \quad \text{Legendre}$$

$$\alpha_{N+1}(x) \equiv T_{N+1}(x) \quad \text{Chebyshev}$$

$$\alpha_{N+1}(x) \equiv H_{N+1}(x) \quad \text{Hermite}$$

i.e. If we choose the x_i to be the zeros of these polynomials then we obtain Gauss-Legendre, Gauss-Chebyshev or Gauss-Hermite integration.

e.g. Gauss-Chebyshev:

$$w(x) = \frac{1}{\sqrt{1-x^2}}$$

$$\int_{-1}^{1} f(x)w(x)dx = \sum_{i=0}^{N} a_i f(x_i)$$

leads to

$$P(x) = \sum_{i=0}^{N} \frac{T(x)}{(x-x_i)T'(x_i)} f(x_i)$$

$$a_i = \int_{-1}^{1} \frac{T(x)}{(x-x_i)T'(x_i)} w(x)$$

Recall

$$a_i = \int_{-1}^{1} \frac{\alpha(x)}{(x - x_i)\alpha'(x_i)} w(x)$$

Consider Gauss-Legendre $\alpha \to L_N$

$$w(x) = 1$$

Therefore

$$a_i = \int_{-1}^{1} \frac{L_N(x)}{(x - x_i)L'_N(x_i)} dx$$

(Here L'_N refers to the derivative).

The *Christoffel-Darbour* identity is:

$$(x - x') \sum_{k=0}^{N} P_k(x) P_k(x') = \frac{\Theta_N}{\Theta_{N+1}} \left[P_{N+1}(x) P_N(x') - P_N(x) P_{N+1}(x') \right]$$

Here P are *orthonormal.*

At $x' = x_i$, where x_i are zeros of P_N, so,

$$P_N(x_i) = 0.$$

We have

$$\sum_{k=0}^{N} P_k(x) P_k(x_i) = -\frac{\Theta_N}{\Theta_{N+1}} \frac{P_N(x) P_{N+1}(x_i)}{(x - x_i)}$$

Θ_N is the coefficient of x^N in $P_N(x)$.

Multiply by $w(x)$ and integrate over the interval,

$$\int_{-1}^{1} \sum_{k=0}^{N} P_k(x) P_k(x_i) w(x) = -\frac{\Theta_N}{\Theta_{N+1}} \int_{-1}^{1} \frac{P_N(x) P_{N+1}(x_i)}{(x - x_i)} w(x) dx$$

$$\sum_{k=0}^{N} P_k(x_i) \int_{-1}^{1} P_k(x) w(x) = -\frac{\Theta_N}{\Theta_{N+1}} P_{N+1}(x_i) \int_{-1}^{1} \frac{P_N(x) w(x)}{(x - x_i)} dx$$

The LHS is 1 if $k = 0$ and 0 if $k \neq 0$ (orthonormality of P_N).

Hence

$$1 = -\frac{\Theta_N}{\Theta_{N+1}} P_{N+1}(x_i) \int_{-1}^{1} \frac{P_N(x) w(x)}{(x - x_i)} dx$$

Thus

$$a_i = \int_{-1}^{1} \frac{P_N(x)}{(x - x_i) P'_N(x_i)} w(x) dx$$

$$= \frac{1}{P'_N(x_i)} \int_{-1}^{1} \frac{P_N(x)}{(x - x_i)} w(x) dx$$

$$a_i = -\frac{\Theta_{N+1}}{\Theta_N} \frac{1}{P'_N(x_i) P_{N+1}(x_i)}$$

for Legendre polynomials, orthonormality gives

$$\Theta_N = \sqrt{\frac{2N+1}{2}} \frac{(2N)!}{2^N (N!)^2}$$

(Note, $\hat{L}(x) = \sqrt{\frac{2n+1}{2}} L(x)$)

Hence

$$a_i = -\frac{2}{(N+1)L'(x_i)L_{N+1}(x_i)}$$

Also:

$$(1-x^2)L'_N(x) = (N+1)\left[xL_N(x) - L_{N+1}(x)\right]$$

for $x = x_i$

$$(1-x_i^2)L'_N(x_i) = (N+1)\left[x_iL_N(x_i) - L_{N+1}(x_i)\right]$$

or

$$L_{N+1}(x_i) = -\frac{(1-x_i^2)}{N+1}L'_N(x_i)$$

$$a_i = \frac{2}{(1-x_i^2)\left[L'_N(x_i)\right]^2}$$

which is what is given on p13 with $N \to N+1$.

1.3.1 Lobatto Integration

Unfortunately all of the zeros are in the interior of [-1,1]. So to include these points (for purposes of applying boundary conditions) we must choose as nodes

$$-1,\ x_0,\ x_1,\ \ldots\ x_{N-2},\ +1$$

and thus calculate exactly $f(x) \in \mathcal{P}_{2N-1}$. This is *Gauss-Lobatto Integration*, leading to *Gauss-Legendre-Lobatto Integration*, *Gauss-Chebyshev-Lobatto Integration*, etc.

Should we have included only *one* of the extremal points we would have integration associated with the name of *Radau*.

e.g. Gauss-Legendre-Lobatto, $w(x) = 1$

$$\int_{-1}^{1} f(x)dx = a_0 f(-1) + a_N f(1) + \sum_{k=0}^{N-1} a_i f(x_i)$$

Number of unknowns $(N+1)$ a_i and $(N-1)$ x_i leading to $2N$ unknowns. Hence we can make the formulae exact for $f(x) \in \mathcal{P}_{2N-1}$. Since this is true for all $f(x) \in \mathcal{P}_{2N-1}$, choose $f(x) = x_i \quad i = 0, 1, \ldots$ and get the $2N$ equations

$$a_0 + a_1 + a_2 + \ldots a_N = \int_{-1}^{1} dx = 2$$

$$-a_0 + a_1 x + a_2 x_2 + \ldots a_N = \int_{-1}^{1} x dx = 0$$

$$a_0 + a_1 x_1^2 + a_2 x_2^2 + \ldots a_N = \int_{-1}^{1} x^2 dx = \frac{2}{3}$$

etc.

Solving these will give us the Gauss-Legendre-Lobatto zeros and coefficients.

1.3.2 Sturm-Liouville problem

Legendre and Chebyshev polynomials are examples of *Jacobi Polynomials* which are eigenfunctions of the *singular Sturm-Liouville problem*:

$$-\frac{d}{dx}\left(p(x)\frac{du}{dx}\right) + q(x)u = \lambda w(x)u \quad \text{on}[-1, 1]$$

Here p, q, w are real and $w(x)$ is a "weight".

The singular problem is when $p(\pm 1) = 0$

$$w(x) = (1-x)^{\alpha}(1+x)^{\beta}$$

	$\alpha = 0$	$\alpha = \beta = \frac{1}{2}$
	Legendre	Chebyshev
λ	$-k(k+1)$	$-k^2$
$p(x)$	$1-x^2$	$(1-x^2)^{\frac{1}{2}}$
$q(x)$	0	0
$w(x)$	1	$(1-x^2)^{\frac{1}{2}}$

Table 3: Legendre and Chebyshev polynomials as eigenfunctions of the Sturm-Louiville problem as defined here.

1.3.3 Summary of Basis Function Properties

LEGENDRE

$$L_0(x) = 1, L_1(x) = x, L_2(x) = \frac{1}{2}(3x^2 - 1), L_3(x) = \frac{1}{2}(5x^3 - 3x^2),$$

$$L_4(x) = \frac{1}{8}(35x^4 - 30x^2 + 3)$$

Orthogonality

$$\int_{-1}^{1} L_k(x)L_l(x)dx = \frac{1}{\sqrt{k+\frac{1}{2}}}\delta_{kl}$$

Recurrence

$$L_{k+1}(x) = \frac{2k+1}{k+1}xL_k(x) - \frac{k}{k+1}L_{k-1}(x)$$

Gauss-Legendre

$$x_i \text{ zeros of } L_{N+1},\ w_i = \frac{2}{(1-x_i^2)\left[L'_{N+1}(x_i)\right]^2}, \quad i = 0, 1, \ldots N$$

Gauss-Legendre-Lobatto

$$x_0 = -1, x_N = 1,\ x_i \text{zeros of } L'_N, \quad i = 0, 1, \ldots N-1$$

$$w_i = \frac{2}{N(N+1)} \frac{1}{[L_N(x_i)]^2} \quad i = 0, 1, \ldots N$$

Differentiation

$$\text{If } u = \sum_{i=0}^{\infty} \hat{u} L_i, \; u' = \sum_{i=0}^{\infty} u_i^{(1)} L_i, \quad \text{where } u_i^{(1)} = (2i+1) \sum_{p=i+1 p+i \text{odd}}^{\infty} \hat{u}_p$$

Interpolation (GLL)

$$P_i(x) = \frac{1}{N(N+1)L_N(x_i)} \frac{(1-x^2)L'_N(x)}{(x-x_i)}$$

CHEBYSHEV POLYNOMIALS

$$T_0(x) = 1, \; T_1(x) = x, \; T_2(x) = 2x^2 - 1, \; T_3(x) = 4x^3 - 3x,$$

$$T_4(x) = 8x^4 - 8x^2 + 1$$

Orthogonality

$$\int_{-1}^{1} \frac{T_k(x) T_l(x)}{\sqrt{1-x^2}} dx = C_k \delta_{kl} \frac{\pi}{2}, \quad \text{where } C_k = 2, k = 0 \text{ and } C_k = 1, k \geq 1$$

Recurrence

$$T_{N+1}(x) = 2x T_N(x) - T_{N-1}(x)$$

Gauss-Chebyshev

$$\xi_i = \cos \frac{(2i+1)\pi}{2N+2}, \quad w_i = \frac{\pi}{N+1}$$

Gauss-Chebyshev-Lobotto

$$x_i = \cos\frac{\pi i}{N}, \quad w_i = \frac{\pi}{2N} \quad i = 0, 1, \ldots N, \quad w_i = \frac{\pi}{N} i \leq i \leq N-1$$

Differentiation

$$\text{If} \quad u = \sum_{i=0}^{\infty} \hat{u} T_i, u' = \sum_{i=0}^{\infty} u_i^{(1)} T_i, \qquad \text{where } u_i^{(1)} = \frac{2}{C_i} \sum_{\substack{p=i+1 \\ p+i \text{ odd}}}^{\infty} \hat{p} u_p$$

Interpolation (GCL)

$$P_i(x) = \frac{(-1)^i + 1(1-x^2)T_N'(x)}{\bar{C}_i N^2 (x - x_i)} \qquad \begin{cases} \bar{C}_i = 2 & i = 0 \\ \bar{C}_i = 1 & i \neq 0 \end{cases}$$

1.4 Method of Weighted Residuals

Consider

$$\frac{\partial u}{\partial t} = D(x)$$

$$u_N(x,t) = \sum_{i=0}^{N} a_i(t)\phi(x)$$

Here a_i are the *expansion coefficients*, ϕ are the *trial or expansion functions*

Then

$$R_N = \frac{\partial u_N}{\partial t} - D(u_N)$$

is the *Residual.*

The *Method of Weighted Residuals* is to minimize the residual by

$$\int_a^b R_N \psi_j(x) dx = 0 \quad j = 0, 1, \ldots N$$

The *Galerkin method* follows when $\phi(x) \equiv \psi(x)$ and they satisfy the boundary conditions. The *Collocation Method* follows when $\psi(x) \equiv \delta(x)$, and the *Tau method* follows when $\phi(x) \equiv \psi(x)$ but they do not satisfy the boundary conditions.

Galerkin Example: Fourier Galerkin

$$\frac{\partial u}{\partial t} = \frac{\partial u}{\partial x} \quad \partial\Omega = [0, 2\pi] \quad \text{wave equation}$$

$$\phi_k(x) = e^{ikx}$$

$$\psi_k(x) = \frac{1}{2\pi} e^{-ikx}$$

MWR impies

$$\frac{1}{2\pi} \int_0^{2\pi} \left[\sum_{k=0}^{N} (\dot{a}_k - ika_k) e^{ikx} \right] e^{-ilx} dx = 0$$

$$\frac{da_k}{dt} - ika_k = 0 \quad k = 0, 1, \ldots N$$

These $N + 1$ equations can be solved using any reasonable time integration scheme.

Another example

$$\nabla^2 u = f$$

$$\text{with} \quad u = 0 \quad \text{on } \partial\Omega$$

$$\phi_k(x) = T_k(x) - T_0(x) \quad k \text{ even}, \quad T_k(x) - T_1(x) \quad k\text{odd}$$

We could also use Legendre.

$$u_N = \sum_{l=0}^{N} a_{kl}\phi_k$$

$$\int_\Omega \nabla^2 u_N \phi_{kl} w(x,y)dxdy = \int f\phi_{kl} w(x,y)dxdy$$

Rest is algebra.

Collocation Example Chebyshev

$$\frac{\partial u}{\partial t} = \frac{\partial^2 u}{\partial x^2} \quad u(\pm 1, t) = 0 \quad \text{diffusion equation}$$

$$\phi(x) = T_k(x) \quad k = 0, 1, \ldots N$$

$$u_N(x,t) = \sum_{k=0}^{N} a_k(t)\phi(x)$$

$$\psi_j(x) = \delta(x - x_j) \quad j = 1, 2, \ldots N$$

here x_j are *collocation points.*

MWR implies

$$\int_{-1}^{1} \left[\frac{\partial u_N}{\partial t} - \frac{\partial^2 u_N}{\partial x^2}\right] \psi_j(x)dx = 0$$

or

$$\frac{\partial u_N}{\partial t} - \frac{\partial^2 u_N}{\partial x^2}|_{x=x_j} = 0 \quad j = 1, 2, \ldots N \quad + \text{B.C.}$$

Choose $x_j = \cos\frac{\pi j}{N}$, and note $\phi_k(x_j) = \cos\frac{\pi j}{N}$. Use FFT to find $\frac{\partial^2 u_N}{\partial x^2}|_{x=x_j}$.

$$\frac{\partial^2 u_N}{\partial x^2} = \sum_{k=0}^{N} a_k^{(2)}(t) T_k(x)$$

So

$$\frac{\partial u_N}{\partial t}|_{x=x_j} = \sum_{k=0}^{N} a_k^{(2)} \cos\frac{\pi jk}{N}$$

Another **Collocation example**

$$-\nu\frac{\partial^2 u}{\partial x^2} + u = f \quad x \in [-1,1] \quad \text{Helmholtz equation}$$

$$u(-1) = \alpha, \quad u(1) = \beta \quad \text{boundary conditions}$$

Let

$$u_N(x) = \sum_{k=0}^{N} \hat{u}_k T_k(x) \quad \text{Chebyshev}$$

$$u_j = \cos\frac{\pi j}{N}$$

$$R_N(x_j) = -\nu\frac{\partial^2 u_N}{\partial x^2}(x_j) + u_N(x_j) - f(x_j)$$

MWR: Residual is zero at x_j

$$\frac{\partial^2 u_N}{\partial x^2}(x_j) = \sum_{l=0}^{N} d_{lj} u_N(x)$$

Recall

$$u'_N(x_i) = \sum_{l=0}^{N} \hat{u}_k^{(1)} T_k(x_i)$$

$$\hat{u}_k^{(1)} = \frac{2}{\bar{c}_k} \sum_{\substack{p=k+1 \\ p+k\text{odd}}}^{N} p\hat{u}_p$$

$$u'_N(x_i) = \sum_{k=0}^{N} \left[\frac{2}{\bar{c}_k} \sum_{p} p\hat{u}_p \right] T_k(x_i)$$

But

$$\hat{u}_p = \frac{2}{\bar{c}_p N} \sum_{i=0} \frac{1}{\bar{c}_i} u_i T_k(x_i)$$

so

$$u'_N(x_i) = \sum_{j=0}^{N} d_{ij}^{(1)} u_j \quad (u_j = u_N(x_j))$$

and

$$u''_N(x_i) = \sum_{j=0}^{N} d_{ij}^{(2)} u_j.$$

So returning to the example, we obtain:

$$-\nu \sum_{l=0} d_{jl} u_N(x_l) + u_N(x_j) - f(x_j) = 0 \quad j = 1, 2, \ldots N-1$$

$$u_N(-1) = \alpha \quad u_N(1) = \beta$$

This algebraic system of equations has the $N-1$ unknowns, $u_N(x_j), \quad j = 1, 2, \ldots N-1$.

Yet another **Collocation example**.

$$\frac{\partial}{\partial x}\left(\alpha(x)\frac{\partial u}{\partial x}\right) = f \quad x \in [-1,1] \quad \text{variable coefficient example}$$

with boundary condition

$$u(\pm 1) = 0$$

Collocation implies

$$\frac{d}{dx} I_N \left(\frac{d}{dx} u_N(x_k)\right) = f(x_k) \quad k = 1, 2, \ldots N-1$$

$$u_N(x_0) = u_N(x_N) = 0$$

Where I_N is the Chebyshev or Legendre interpolation operator on the x_k points.

Tau method example

$$\frac{\partial u}{\partial t} = \frac{\partial u}{\partial x} \quad x \in [-1,1]$$

with boundary conditions

$$u(x,0) = \alpha(x) \quad u(1,t) = \beta(t)$$

$$u_N = \sum_{k=0}^{N} a_k(t) T_k(x)$$

As we have done before in the Galerkin example with the same equation but different boundary conditions, we will obtain equations

$$\frac{da_k}{dt} = A_{kl}a_l \quad k,l = 0,1,\ldots N \tag{1}$$

But also have

$$\sum_{k=0}^{N} a_k(t)T_k(1) = \beta(t) \tag{2}$$

Noting that the $u(x,0) = \alpha(x)$ since initial condition is no problem, initial values of coefficients can be taken as Chebyshev coefficients.

Essence of the Tau method is to drop one of the equations in (1) and satisfy (2)

What is to guide the choice of which equation in (1) to discard? For Chebyshev polynomials note that a derivative reduces order. Therefore equating terms of same T_k (or equivalently, invoking orthogonality) will lead to deficiency for a_N if only 1st derivative occurs, etc. In our example $\frac{da_N}{dt} = 0$, because we have a 1st derivative (in x). Hence we can safely discard this equation for (2).

Another Tau example[1]

$$\nu\frac{d^2u}{dx^2} - \lambda u = f \quad x \in [-1,1]$$

$$u(-1) = \alpha \quad u(1) = \beta$$

$$u_N = \sum_{k=0}^{N} \hat{u}_k T_k(x), \quad f_N(x) = \sum_{k=0}^{N} \hat{f}_k T_k(x)$$

MWR implies

$$\int_{-1}^{1} \left(\frac{d^2u_N}{dx^2} - \lambda u_N \right) T_k(x)w(x)dx = \int_{-1}^{1} f_N(x)T_k(x)w(x)dx \quad k = 0,1,\ldots N-1$$

[1]This example is due to R. Peyret.

or

$$\nu \hat{u}_k^{(2)} - \lambda \hat{u}_k = \hat{f}_k, \quad k = 0, 1, \ldots N-2$$

$$\sum_{k=0}^{N} (-1)^k \hat{u}_k = \alpha, \quad \sum_{k=0}^{N} \hat{u}_k = \beta$$

Which is a total of N equations.

The system (1) has

$$\hat{u}_k^{(2)} = \frac{1}{c_k} \sum_{\substack{p=k+2 \\ p+k \text{ even}}} p(p^2 - k^2)\hat{u}_p$$

Hence looks like

$$\frac{\nu}{c_k} \sum_{\substack{p=k+2 \\ p+k \text{ even}}} p(p^2 - k^2)\hat{u}_p - \lambda \hat{u}_k = \hat{f}_k \quad k = 0, 1, \ldots N-2$$

+ 2 equations for boundary conditions. Written out this is ($\nu = 1$):

$$\begin{array}{llllll}
\hat{f}_0 = & -\frac{\lambda}{2}\hat{u}_0 & & +\frac{2(2^2)}{2}\hat{u}_2 & & +\frac{4(4^2)}{2}\hat{u}_4 \\
\hat{f}_1 = & & -\lambda \hat{u}_1 & & +3(3^2-1)\hat{u}_3 & & +5(5^2-1)\hat{u}_5 \\
\hat{f}_2 = & & & -\frac{\lambda}{2}\hat{u}_2 & & +4(4^2-2^2)\hat{u}_4 & \\
\hat{f}_3 = & & & & -\lambda \hat{u}_3 & & 5(5^2-3^2)\hat{u}_5
\end{array}$$

This is of form $LU = F$ where L is upper triangular. But solving it this way is inefficient ($O(N^2)$ operations). Instead, note the alternating zeros. Therefore we can uncouple odd and even modes. [In between apply complicated recurrence relation to obtain qusi-tridiagonal system.]

The boundary conditions look like

$$\hat{u}_0 - \hat{u}_1 + \hat{u}_2 \cdots \hat{u}_N = \alpha$$

$$\hat{u}_0 + \hat{u}_1 + \hat{u}_2 \cdots \hat{u}_N = \beta$$

Adding and subtracting

$$\hat{u}_0 + \hat{u}_2 + \cdots \hat{u}_N = \frac{(\alpha + \beta)}{2}$$

$$\hat{u}_1 + \hat{u}_3 + \cdots \hat{u}_{N-1} = \frac{(\alpha - \beta)}{2}$$

So that two systems need to be solved.

$$\boldsymbol{M}_e \hat{\boldsymbol{U}}_e = \boldsymbol{F}_e$$

and

$$\boldsymbol{M}_o \hat{\boldsymbol{U}}_o = \boldsymbol{F}_o$$

$$\hat{\boldsymbol{U}}_e = \begin{pmatrix} \hat{u}_0 \\ \hat{u}_2 \\ \hat{u}_4 \\ \cdots \\ \hat{u}_N \end{pmatrix}$$

$$\hat{\boldsymbol{U}}_o = \begin{pmatrix} \hat{u}_1 \\ \hat{u}_3 \\ \hat{u}_5 \\ \cdots \\ \hat{u}_{N-1} \end{pmatrix}$$

$$\boldsymbol{M}_{e,o} = \begin{pmatrix} 1 & 1 & 1 & \cdots & 1 \\ \times & \times & \times & . & . \\ . & \times & \times & \times & . \\ . & . & \times & \times & \times \\ . & . & . & \times & \times \end{pmatrix}$$

1.5 The Fourier Basis and the FFT

There are two conventions prevalent for defining the Fourier transfom. The *Physical sciences convention* (Press et al. , Mathematica),

Physical	Spectral
$u_j = \frac{1}{N}\sum_{k=0}^{N-1} \hat{u}_k e^{-i2\pi kj/N}$	$\hat{u}_k = \sum_{j=0}^{N-1} u_j e^{i2\pi kj/N}$

Here $\hat{u}_k$ are the Fourier coefficients and u_k and $\hat{u}_k$ are reffered to as Fourier transform pairs.

and the *Engineering convention* (Canuto et al. , Strang, Temperton),

Physical	Spectral
$u_j = \sum_{k=0}^{N-1} \hat{u}_k e^{i2\pi kj/N}$	$\hat{u}_k = \frac{1}{N}\sum_{j=0}^{N-1} u_j e^{-i2\pi kj/N}$

Fourier transforms are appropriate for periodic systems. They satisfy the orthogonality condition,

$$\frac{1}{N}\sum_{j=0}^{N-1} e^{ipx_j} = \begin{cases} 1 & p = Nm \quad m = 0, 1, \ldots \\ 0 & p \neq Nm \quad m = 0, 1, \ldots \end{cases}$$

with $x_j = \frac{2\pi j}{N} \quad j = 0, 1, \ldots N-1$

Note that

$$I_N u(x) = \sum_{k=0}^{N-1} \hat{u}_k e^{ikx}$$

is an $N/2$ degree trignometric interpolant of u. i.e.

$$I_N u(x_j) = u(x_j)$$

It is of degree $N/2$ because u and $\hat{u}$ are complex here.

An important point to note is that this is different from truncating the (infinite) Fourier series representation of the function,

$$u(x) = \sum_{k=-\infty}^{\infty} a_k e^{ikx}$$

if we truncate this,

$$u(x) = \sum_{k=-N/2}^{N/2-1} a_k e^{ikx} \left(= \sum_{k=0}^{N-1} a_k e^{ikx} \quad \text{see below} \right)$$

$$a_k \neq \hat{u}_k$$

1.5.1 Aliasing

The $\hat{u}_k$ can be expressed in terms of the a_k as

$$\hat{u}_k = a_k + \sum_{m=-\infty}^{\infty} a_{k+Nm} \quad k = 0, 1, \ldots N-1 \tag{3}$$

To see this consider

$$u = \sum_{p=-\infty}^{\infty} a_p e^{ipx}, \qquad u_N = \sum_{k=-N/2}^{N/2-1} \hat{u}_k e^{ikx}$$

$$u(x_j) = u_N(x_j) = \sum_{p=-\infty}^{\infty} a_p e^{ipx_j} = \sum_{k=-N/2}^{N/2-1} \hat{u}_k e^{ikx}$$

$$\left(\sum_{p=-\infty}^{-N/2} a_p e^{ipx_j} + \sum_{p=N/2}^{\infty} a_p e^{ipx_j} \right) + \sum_{p=-N/2}^{N/2-1} a_p e^{ipx_j} = \sum_{k=-N/2}^{N/2-1} \hat{u}_k e^{ikx}$$

$$\left(\sum_{m=-\infty}^{\infty} a_{k+Nm} e^{i(k+Nm)x_j}, \quad k = -N/2, \ldots, N/2-1 \right) + \sum_{p=-N/2}^{N/2-1} a_p e^{ipx_j} = \sum_{k=-N/2}^{N/2-1} \hat{u}_k e^{ikx}$$

but $e^{i(k+Nm)x_j} = e^{ikx_j}$, and hence term by term equality leads to (3).

We have generally "slid" the wavenumber limits to range from $k = 0, \ldots, N$ rather than from $k = -N/2, \ldots, N/2 - 1$ because of this aliasing. The coefficients from $N/2$ to $N - 1$ are the same as those from $-N/2$ to -1.

Now (3) can be thought of as

$$I_N u = P_N u + R_N u$$

Where I_N is the *interpolating operator*, P_N is the *projection operator*, and R_N is the *aliasing error operator*.

Thus the $(K + Nm)$-th frequency aliases the k-th frequency on the grid. On the x_j nodes $\phi_{k+Nm}(x_j) = \phi_k(x_j)$

Also note

$$\|u - I_N u\|^2 = \|u - P_N u\|^2 + \|R_N u\|^2$$

or

interpolation error = truncation error + aliasing error

Thus interpolation error is always greater thatn the truncation error. Asymptotically however both errors are of the same order and decay at the same rate. Thus Galerkin and Collocation methods have similar approximation errors.

Fourier coefficients decay with k in the following manner.

for $u \in C^m$ (u is m times differentiable)

$$a_k = O(k^{-m}) \quad j = 0, 1, \ldots N - 1$$

So for C^∞ functions, the k-th coefficient decays faster than any algebraic power of $\frac{1}{k}$. Because of relationship between $\hat{u}_k$ and a_k, a similar statement is true for $\hat{u}_k$.

1.5.2 Differentiation

In *transform space*

$$u' = \sum_{k=0}^{N} ika_k e^{ikx}$$

Hence

$$(\mathcal{P}_N u)' = \mathcal{P}_N u'$$

This means that *truncation and differentiation commute* for Fourier basis. In *physical space*

$$D_N u = (I_N u)'$$

$$D_N u \neq \mathcal{P}_N u'$$

so that

$$(I_N u)' \neq I_N u'$$

Interpolation and differentiation do not commute. But it is found that the collocation differentiation error

$$(I_N u)' - I_N u' \approx O(u' - P_N u')$$

where the RHS represents the trunucation error of the derivative.

Hence is spectrally accurate.

1.5.3 The Fast Fourier Transform

If we write

$$\omega = e^{-2\pi i/N}$$

then

$$\hat{u}_k = \frac{1}{N} \sum_{j=0}^{N-1} \boldsymbol{\omega}^{jk} u_j$$

where $\boldsymbol{\omega}$ is a matrix and u_j is a vector. A direct calculation would take $O(N^2)$ operations.

But with the discovery of the FFT, this can be considerably reduced.

$$\sum_{j=0}^{N-1} \boldsymbol{\omega}^{jk} u_j = \sum_{j=0}^{N-1} e^{-2\pi ijk/N} u_j$$

$$= \sum_{j=0}^{N/2-1} e^{-2\pi i(2J)k/N} u_{2j} + \sum_{j=0}^{N/2-1} e^{-2\pi i(2j+1)k/N} u_{2j+1}$$

$$\sum_{j=0}^{N/2-1} e^{-2\pi ikj/(N/2)} + \omega^k \sum_{j=0}^{N/2-1} e^{-2\pi ikj/(N/2)} u_{2j+1}$$

or

$$\hat{u}_k = u_k^e + \omega^k u_k^o$$

where u_k^e represents even modes of length $N/2$ and u_k^o the odd modes of length $N/2$. This process can be repeated over and over until one is left with a very short vector lentgh when it makes sense to simply do the matrix multiply. This recursive nature leads to an algorithm that takes $O(N \ln N)$ operations.

1.5.4 The Pseudospectral Method

1.5.5 The `ddcon2d` Code

`ddcon2d`[2] solves the two-dimensional Navier-Stokes equations for *Boussinesq convection* by Fourier Galerkin + Collocation method. The system models double-diffusive convection in which two agents (e.g. heat and a solute) have opposing contributions to the bouyancy and diffuse at different rates. The problem is of relevance to oceans (heat + salt) and mixing in stars (heat + angular momentum, heat + concentrations etc.) It has been studied extensively in the laboratory, under different guises. The current set up models the occurence of various waves (standing and travelling convection waves)

The equations are

$$\nabla \cdot \boldsymbol{u} = 0 \tag{4}$$

$$\frac{\partial \boldsymbol{u}_i}{\partial t} - (\boldsymbol{u} \times \boldsymbol{\omega})_i = -\nabla(p + \frac{1}{2}|u^2|) + \sigma(T + S)\delta_{i3} + \sigma\nabla^2 u_i \tag{5}$$

$$\frac{\partial T}{\partial t} + \boldsymbol{u} \cdot \nabla T = R_T w + \nabla^2 T \tag{6}$$

$$\frac{\partial S}{\partial t} + \boldsymbol{u} \cdot \nabla S = -R_S w + \tau\nabla^2 S \tag{7}$$

The second term on the RHS of (5) is the *bouyancy term*, $\boldsymbol{\omega}$ is the vorticity.

The velocity, $\boldsymbol{u} = \{u, w\}$. R_T and R_S are the thermal and solutal *Rayleigh numbers*,

$$R_T = \frac{g\alpha\frac{\partial T}{\partial z}h^4}{\nu\kappa_T}$$

$$R_S = \frac{g\alpha\frac{\partial S}{\partial z}h^4}{\nu\kappa_S}$$

[2]The code may be obtained from my web site at *http://sdcd.gsfc.nasa.gov/ESS/deane.html.*

σ is the *Prandtl number*, and

$$\tau = \kappa_T/\kappa_S \leq 1$$

The "opposing contribution" reffered to in the previous paragraph is seen in the sign of the $R_T w$, $R_S w$ terms. One other dimensionless parameter is a the *aspect ratio* of the domain.

We write

$$\hat{u} = \frac{1}{N_x N_z} \sum_{k_x k_z} u e^{ik_x 2\pi x/N_x} \cos(\pi k_z z/N_z)$$

$$\hat{T} = \frac{1}{N_x N_z} \sum_{k_x k_z} T e^{ik_x 2\pi x/N_x} \sin(\pi k_z z/N_z)$$

$$\hat{S} = \frac{1}{N_x N_z} \sum_{k_x k_z} S e^{ik_x 2\pi x/N_x} \sin(\pi k_z z/N_z)$$

$$\hat{w} = \frac{1}{N_x N_z} \sum_{k_x k_z} w e^{ik_x 2\pi x/N_x} \sin(\pi k_z z/N_z)$$

Take $\nabla\times$ (5) and apply (4) to obtain

$$-\frac{\partial}{\partial x_i}(u \times \omega)_i = -\frac{\partial^2}{\partial x_i^2} q + \sigma(\frac{\partial T}{\partial t} + \frac{\partial S}{\partial t})\delta_{i3}$$

where $q = p + \frac{1}{2}|\boldsymbol{u}|^2$ and denote $(u \times \omega)_i$ by ζ_i.

Fourier transforming

$$-ik_i\hat{\zeta}_i = |\boldsymbol{k}|^2 \hat{q} + i\sigma k_i(\hat{T} + \hat{S})\delta_{i3}$$

so that

$$\hat{q} = \frac{1}{|k|^2}(-ik_i\hat{\zeta}_i - i\sigma k_i(\hat{T} + \hat{S})\delta_{i3})$$

Fourier transform (5), (6),(7) we obtain

$$\frac{\partial}{\partial t}\hat{u}_i - \hat{\zeta}_i = -ik_i\hat{q} + \sigma(\hat{T} + \hat{S})\delta_{i3}) - |k|^2\hat{T}$$

$$\frac{\partial \hat{T}}{\partial t} + \widehat{u \cdot \nabla T} = R_T\hat{w} - |k|^2\hat{T}$$

$$\frac{\partial \hat{S}}{\partial t} + \widehat{u \cdot \nabla S} = -R_S\hat{w} - \tau|k|^2\hat{S}$$

In *pseudospectral method* evaluate nonlinear term in physical space (collocation) rest in spectral space (Galerkin).

We use a leap-frog method for time integration.

$$\frac{u^{n+1} - u^{n-1}}{2\Delta t} = \mathcal{D}_{NL}$$

for the nonlinear term, represented by $\mathcal{D}_{NL}$.

And we use Crank-Nicolson for the diffusion term.

$$\frac{u^{n+1} - u^{n-1}}{2\Delta t} = \frac{1}{2}(\nabla^2 u^{n+1} + \nabla u^{n-1})$$

Discrete equations are

$$\frac{\hat{u}_i^{n+1} - \hat{u}_i^{n-1}}{2\Delta t} - \hat{\zeta}_i^n = ik_i\hat{q}^n + \sigma(\hat{T}^n + \hat{S}^n)\delta_{i3} - \frac{1}{2}\sigma|k|^2(\hat{u}_i^{n+1} - \hat{u}_i^{n-1})$$

$$\frac{\hat{T}_i^{n+1} - \hat{T}_i^{n-1}}{2\Delta t} + ik_i(\widehat{u \cdot T})_i^n = R_T w^n - \frac{1}{2}|k|^2(\hat{T}_i^{n+1} - \hat{T}_i^{n-1})$$

$$\frac{\hat{S}_i^{n+1} - \hat{S}_i^{n-1}}{2\Delta t} + ik_i(\widehat{u \cdot S})_i^n = -R_S w^n - \frac{\tau}{2}|k|^2(\hat{S}_i^{n+1} - \hat{S}_i^{n-1})$$

Let

$$\hat{\alpha}_i = u_i^{n-1}(1 - \sigma|k|^2\Delta t) + 2\Delta t\hat{\zeta}_i^n + 2\sigma\Delta t(\hat{T}^n + \hat{S}^n)\delta i3$$

so that

$$\hat{u}_i^{n+1}(1 + \sigma\Delta t|k|^2) = \hat{\alpha}_i - \frac{1}{|k|^2}k_i(\boldsymbol{k} \cdot \hat{\alpha})$$

since $k_i \cdot u_i = 0$ (from continuity).

Therefore the numerical iteration is

$$\hat{\alpha_x} = \hat{u}^{n-1}(1 - \sigma\Delta t|k|^2) + 2\Delta t\hat{\zeta}_x^n$$

$$\hat{\alpha_z} = \hat{w}^{n-1}(1 - \sigma\Delta t|k|^2) + 2\Delta t\hat{\zeta}_z^n + 2\Delta t\sigma(\hat{T}^n + \hat{S}^n)$$

$$\hat{u}^{n+1} = \frac{\left[\hat{\alpha}_x - k_x\frac{(k\cdot\hat{\alpha})}{|k|^2}\right]}{(1 + \sigma\Delta t|k|^2)}$$

$$\hat{w}^{n+1} = \frac{\left[\hat{\alpha}_z - k_z\frac{(k\cdot\hat{\alpha})}{|k|^2}\right]}{(1 + \sigma\Delta t|k|^2)}$$

$$\hat{T}^{n+1} = \frac{2\Delta t R_T w^n - i2DT(k \cdot \widehat{uT}^n)}{(1 + \Delta t|k|^2)} + \frac{(1 - \Delta t|k|^2)}{(1 + \Delta t|k|^2)}T^n$$

$$\hat{S}^{n+1} = \frac{-2\Delta t R_S w^n - i2DT(k \cdot \widehat{uS}^n)}{(1 + \Delta t\tau|k|^2)} + \frac{(1 - \Delta t\tau|k|^2)}{(1 + \Delta t\tau|k|^2)}S^n$$

All transforms are done using Temperton FFT packages `cf99F` and `ff99f`.

Data is manipuated in the routines in `fft32.f` to perform the necessary two-dimensional transforms.

`SIZE` size of system

`ddcon2d.dat` input parameters

`ddcon2d.f` solver

`fft32.f` array manipulating routines for use with the FFTs

`fft99f.f, cfft99f.f` Temperton FFT routines

In addition there are two `IDL` routines for visulaization of data:

`vector.pro` plays "movie" of data.

`time.pro` reads and plots time traces of $\boldsymbol{u}$.

There is also a `README` file.

1.6 Temporal Discretization

We have been discussing the solution of PDEs using spectral techniques. The discussion till now has focused on the application of spectral methods to the discretization of the spatial component of the PDE. The time advancement techniques commonly employed are almost invariably finite difference. The evaluation of the spatial operator at multiple time levels is expensive to compute and store and temporal discretizations tend to be low-order.

The chief concerns in time advancement are that of *stability* and convergence. To address these there exists a useful theorm due to Lax, namely,

Lax Equivalence Theorm: stability + consistency = convergence.

The stability of any numerical scheme is strongly influenced by the eigenvalue structure of the spatial discretization matrix. To see this we write

$$\frac{\partial \boldsymbol{U}}{\partial t} = \boldsymbol{S}\boldsymbol{U} + \boldsymbol{Q}$$

Here S contains the spatial discretization, and Q are any nonhomogeneous or boundary terms, while U is the vector of mesh point values.

The exact solution is directly determined by the eigenstructure of S.

Characteristic equation is

$$|S - \lambda I| = 0$$

If V_j are the eigenvectors corresponding to λ_j, implies

$$SV_j = \lambda V_j$$

and

$$SR = R\Lambda$$

where

$$\Lambda = \begin{pmatrix} \lambda_1 & & & & \\ & \lambda_2 & & & \\ & & . & & \\ & & & . & \\ & & & & \lambda_N \end{pmatrix}$$

so that

$$\Lambda = R^{-1}SR$$

Since V_j are complete we can write ($\hat{U}$ is exact solution of equation),

$$\hat{U} = \sum_{j=1}^{N} \hat{U}_j(t) V_j$$

and

$$Q = \sum_{j=1}^{N} Q_j V_j$$

$$\hat{U}_j \quad \text{is obtained from} \quad \frac{\partial \hat{U}}{\partial t}_j = \lambda_j \hat{U}_j + Q_j$$

Formally the solution will look like

$$\hat{U}(t) = \sum_{j=1}^{N} \left[U_{0j} e^{\lambda_j t} + \frac{Q_j}{\lambda_j} (e^{\lambda_j t} - 1) \right] V_j$$

Here U_{0j} is the initial condition $U_0 = \sum_{j=1}^{N} U_{0j} V_j$

For $\hat{U}(t)$ to remain bounded

$$\mathrm{Re}(\lambda_j) \leq 0 \quad \forall j$$

[If $\lambda_j = 0$ occurs, it better *not* be multiple, or it will give $\sim te^t$ behavior, leading to asymptotic growth]

Thus as asserted, the eigenstructure of the spatial discretization determines stability; if $\mathrm{Re}(\lambda_j) > 0$ no temporal discretization scheme can be made stable.

Example

$$Lu = \frac{\partial^2 u}{\partial x^2}$$

with either Dirichelet [e.g. $u(\pm 1) = 0$] or Neumann [e.g. $u'(\pm 1) = 0$] boundary conditions.

Using collocation with Gauss-Lobatto points (Chebyshev or Legendre) one finds

$$0 \leq C_1 \leq -\lambda \leq C_2 N^4$$

Another example

$$Lu = \frac{\partial u}{\partial x} \quad \text{with} \quad u(1) = 0$$

Chebyshev Tau gives: $\mathrm{Re}(\lambda) \leq 0$ where $|\lambda| = O(N^2)$ for $N \uparrow$.

Legendre Tau gives: $|\lambda| = O(N^2)$ for $N \uparrow$.

Collocation gives: $|\lambda| = O(N^2)$.

For a temporaly discretized problem,

$$u^{n+1} = z(\lambda)u^n$$

z is amplification factor and will be dependent on λ because of the spatial discretization. We would like $|z| \leq 1$ for a stable scheme.

Example: Leap-Frog

$$u^{n+1} = u^{n-1} + 2\Delta t f^n$$

$$u^{n+1} = u^{n-1} + 2\Delta t \lambda u^n$$

characteristic equation is

$$z = \frac{1}{z} + 2\Delta t \lambda$$

$$\lambda \Delta t = \frac{1}{2}(z - \frac{1}{z})$$

For $z = e^{i\phi}$ $\quad \phi = 0, 2\pi$ gives

$$\lambda \Delta t = i \sin \phi$$

1.6.1 Some Standard Time Stepping Schemes

Leap Frog As described in the previous example,

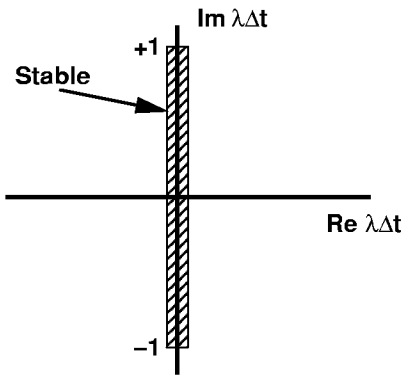

Figure 1: Stability region of the Leap-Frog scheme on the wave equation

$$u^{n+1} = u^{n-1} + 2\Delta t f^n$$

Since stability requires $\mathrm{Re}\lambda\Delta t = 0$ and $|\lambda\Delta t| \leq 1$.

Hence suitable explicit scheme for problems with purely imaginary λ. Good therefore for periodic advection, where eigenvalues of Fourier for $\frac{\partial}{\partial t}$ operator are imaginary.

The scheme requires averaging, as in `ddcon2d`, to prevent disconnected solutions on $2\Delta t$.

For the diffusion operators have $\mathrm{Re}(\lambda) > 0$.

Adams Bashforth. This is a family of schemes.

$$\text{Forward Euler} \quad u^{n+1} = u^n + \Delta t f^n$$

$$\text{AB2} \quad u^{n+1} = u^n + \frac{\Delta t}{2}\left[3f^n - f^{n-1}\right]$$

$$\text{AB3} \quad u^{n+1} = u^n + \frac{\Delta t}{12}\left[23f^n - 16f^{n-1} + 5f^{n-2}\right]$$

$$\text{AB4} \quad u^{n+1} = u^n + \frac{\Delta t}{24}\left[55f^n - 59f^{n-1} + 37f^{n-2} - 9f^{n-3}\right]$$

AB2 and AB4 very popular. For Adams Bashforth schemes the stability region *decreases* with order.

Consider the AB2 scheme

$$z = 1 + \frac{\lambda \Delta t}{2}(3 - \frac{1}{z})$$

or

$$\lambda \Delta t = \frac{2(z-1)}{3 - \frac{1}{z}}$$

alternatively

$$z_\pm = \frac{1}{2}\left(1 + \frac{3}{2}\lambda\Delta t \pm \sqrt{\left[1 + \lambda\Delta t - \frac{9}{4}(\lambda\Delta t)^2\right]}\right)$$

Consider Fourier; e^{ikx}, $\lambda = ik$ and take $\Delta t \to 0$

$$z_k = 1 + ik\Delta t - \frac{1}{2}(k\Delta t)^2 + \cdots$$

$$|z_k| = 1 + \frac{1}{4}(k\Delta t)^4 + O(k^5\Delta t^5)$$

$$|z_k|^{t/\Delta t} \leq \left[1 + \frac{1}{4}(k\Delta t)^4\right]^{t/\Delta t}$$

$$\leq e^{(k^4\Delta t^3)t}$$

Which represents a weak instability. Therefore integrate over a fixed time and keep Δt low.

AB3 and AB4 are stable.

Adams-Moulton An implicit family of schemes.

$$\text{Backwards Euler} \quad u^{n+1} = u^n + \Delta t f^{n+1}$$

$$\text{Crank} - \text{Nicolson} \quad u^{n+1} = u^n + \frac{\Delta t}{2}\left[f^{n+1} + f^n\right]$$

$$\text{AM3} \quad u^{n+1} = u^n + \frac{\Delta t}{12}\left[5f^{n+1} + 8f^n - f^{n-1}\right]$$

Backwards Euler and Crank-Nicolson are *A- Stable*. Crank-Nicolson is very popular for diffusion problems. Adams-Bashforth + Crank-Nicolson for Navier-Stokes are very common. AM3 and AM4 have larger stability region for diffusive problems thatn AB. Weakly unstable for Fourier advection.

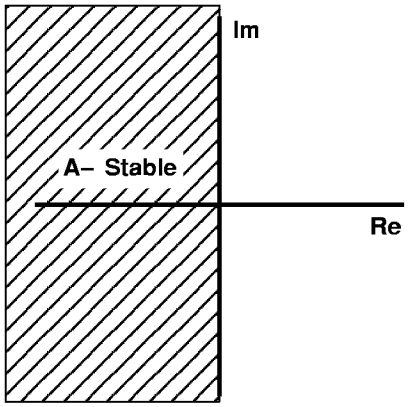

Figure 2: A-Stable region

Runge-Kutta Very useful, very common time advancement schemes.

RK2:

$$\hat{u} = u^n + \alpha \Delta t f^n$$

$$\hat{f} = a f^n + f(\hat{u}, t_n + \alpha \Delta t)$$

$$u^{n+1} = \hat{u} + \frac{\Delta t}{2\alpha} \hat{f}$$

$$a = -1 + 2\alpha - 2\alpha^2$$

$\alpha = \frac{1}{2}$ Modified Euler. RK2 requires only two levels of storage.

RK4: (3 storage level version available)

RK2: Chebyshev collocation for advection

$$\Delta t \leq \frac{16}{N^2} \quad \text{for} \quad N \uparrow$$

2 SPECTRAL ELEMENT METHOD

2.1 Introduction

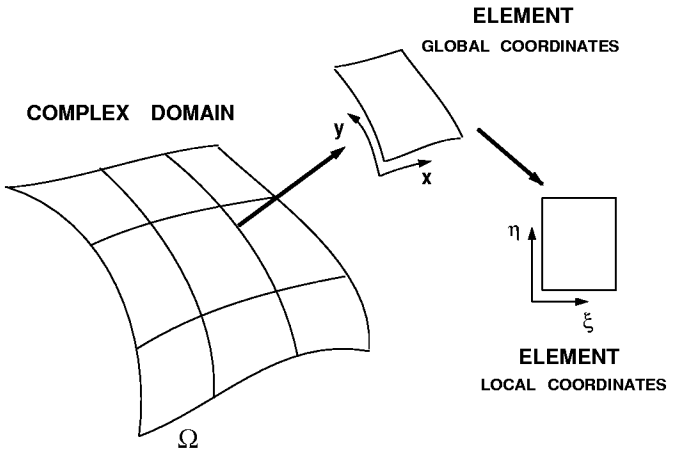

Figure 3: Spectral element discretization

In the Spectral-Element method the physical domain is broken up into several elements, say K in number. Within each element a spectral representation based on N-th order interpolants is used. Spectral Element methods are similar to *p-type* Finite Element methods, but differ in that they use interpolants as trial functions.

$$u_N^k(x) = \sum_{i=0}^{N} u_N^k(x_i) h_i(x)$$

Here $h_i(x)$ is the interpolant.

Until we return to the global coordinates we will use (x, y) to refer to the local coordinates, making it easier to think; rather than confusing relations with spriklings of ξ and η.

Consider the one dimensional Helmholtz equation[3].

[3]This example is from Canuto et al.

$$-u_{xx} + \lambda u = f \quad u(\pm 1) = 0$$

Let there be K 1D elements. In the k-th element

$$x_i^k = \cos \frac{\pi i}{N}, \quad i = 0, 1, \ldots N$$

This is Gauss-Chebyshev-Lobatto. N is degree of polynomial.

MWR implies

$$\sum_{k=1}^{K} \int_{-1}^{1} \left(\frac{\partial u_N}{\partial x} \frac{\partial v}{\partial x} + \lambda u_N v \right) dx = \sum_{k=1}^{K} \int_{-1}^{1} f_N v dx$$

where we have used $\int \frac{\partial^2 u}{\partial x^2} u dx = \int \frac{\partial u}{\partial x} \frac{\partial v}{\partial x} dx$, which involves the boundary condition.

Now

$$h_i(x) = \frac{2}{N} \sum_{j=0}^{N} \frac{1}{\bar{c}_i \bar{c}_j} T_j(x_i) T_j(x)$$

where

$$\bar{c}_p = \begin{cases} 2 & p = 0 \\ 1 & p \neq 0 \end{cases}$$

$$u_N^k = \sum u_N^k(x_i) h_i(x)$$

Take $v \to h_j(x)$

The integral leads to

$$\sum_{j=0}^{N} C_{ij}^k u_j^k = \sum_{j=0}^{N} B_{ij}^k f_j^k$$

$$C_{ij} = A_{ij} + \lambda B_{ij}$$

$$A_{ij} = \frac{8}{N^2}\frac{1}{\bar{c}_i\bar{c}_j}\sum_{n,m=0}^{N}\frac{1}{\bar{c}_n\bar{c}_m}T_n(x_i)T_m(x_j)a_{mn}$$

$$B_{ij} = \frac{2}{N^2}\frac{1}{\bar{c}_i\bar{c}_j}\sum_{n,m=0}^{N}\frac{1}{\bar{c}_n\bar{c}_m}T_n(x_i)T_m(x_j)b_{mn}$$

$$a_{mn} = \int_{-1}^{1}\frac{\partial T_n}{\partial x}\frac{\partial T_m}{\partial x}dx = \begin{cases} 0 & n+m \quad \text{odd} \\ \frac{nm}{2}(J_{(n-m)/2} - J_{(n+m)/2}) & n+m \quad \text{even} \end{cases}$$

Where

$$J_0 = 0, \quad J_k = -4\sum_{q=1}^{k}\frac{1}{2q-1} \quad \text{for} k \geq 1$$

$$b_{nm} = \int_{-1}^{1} T_n T_m dx = \begin{cases} 0 & n+m \text{ odd} \\ \frac{1}{1-(n+m)^2} + \frac{1}{1-(n-m)^2} & n+m \text{ even} \end{cases}$$

A_{ij} is the *stiffness matrix*, B_{ij} is the *mass matrix*.

Actually the test funtion is taken over interior nodes and formulae are more complicated by including the boundaries. But the essentials of the method are here,

$$\boldsymbol{CU} = \boldsymbol{BF}.$$

Let us do a very similar problem, Poisson's equation with Legendre polynomials.

The equation is

$$-u_{xx} = f \quad u(\pm 1) = 0$$

Then again the MWR leads to

$$\int_{-1}^{1} \frac{\partial u}{\partial x}\frac{\partial v}{\partial x}dx = \int_{-1}^{1} f v dx$$

For Legendre recall, $w(x) = 1$

so

$$\int_{-1}^{1} g(x)dx = \sum_{i=0}^{N} a_i g(x_i)$$

$$\sum_{k=1}^{K} a_i \frac{\partial u_N^k(x_i)}{\partial x}\frac{\partial v_N^k(x_i)}{\partial x} = \sum_{k=1}^{K} a_i f^k(x_i) v_N^k(x_i)$$

$$u_N = \sum_{i=0}^{N} u_N(x_i) h_i(x)$$

$$h_i(x) = \frac{1}{N(N+1)L_N(x_i)}\frac{(1-x^2)L'_N(x)}{(x-x_i)}$$

For continuity

$$u_N^k = u_0^{k+1}$$

and because of the homogeneous boundary conditions

$$u_0^1 = u_N^K = 0$$

Now take

$$v_N = h_i(x_j) = \delta_{ij}$$

leading to

$$\sum_{k=1}^{K} A_{ij}^k u_j^k = \sum_{k=1}^{K} B_{ij}^k f_j^k$$

or

$$\boldsymbol{AU} = \boldsymbol{BF}$$

where

$$A_{ij}^k = a_p \frac{\partial h_i}{\partial x}(x_p) \frac{\partial h_j}{\partial x}(x_p) \quad \text{stiffness matrix}$$

$$B_{ij}^k = a_i \delta_{ij}$$

Here the mass matrix is diagonal. This is the advantage of using Legendre basis over, for example, the Chebyshev basis.

2.2 Convergence Character of SEM

For N fixed $K \uparrow$ obtain algebraic convergence. For K fixed $N \uparrow$ obtain exponential (spectral) convergence.

Clearly the advantage of SEM over FEMs is in the exponential convergence. In practice however the *location* of the elements is important too.

For mesh refinement, one can either keep the order fixed and increase the number of elements, or keep the number fixed and increase the order of the method. Additionally one can reposition elements, keeping both K and N fixed, or change N in different elements.

2.3 Multidimensions

For multidimensional problems, every thing follows as described for the one dimensional case described so far. A particularly good feature is that the expansion is in *tensor product* form:

$$u_N^k(x,y) = \sum_{i=0}^{N}\sum_{j=0}^{N} u_{ij}^k h_i(x) h_j(y)$$

This avoids storing the entire transformation matrix. Instead recompute when needed. The two dimensional version of the problem we have looked at is

$$\sum_{k=1}^{N}\left(A_{ip}^k B_{jq}^k + B_{ip}^k A_{jq}^k\right) u_{pq}^k = \sum_{k=1} B_{ip}^k B_{jq}^k f_{pq}^k$$

Where A and B are as for the one-dimensional case.

Can also do mapping of curved domains into cannonical rectangular regions via interpolation.

$$(x,y)_N^k = \sum_i \sum_j (x,y)_{ij}^k h_i(\xi) h_j(\eta)$$

Equations are obviously complicated but the tensor product form is retained. There are extra quadrature errors but these are of same order as approximation errors, for smooth solutions and boundaries.

2.4 Time Splitting for Navier-Stokes

The Navier Stokes equations are:

$$\nabla \cdot \boldsymbol{u} = 0$$

$$\frac{\partial \boldsymbol{u}}{\partial t} = \boldsymbol{u} \times \boldsymbol{\omega} - \nabla p + \frac{1}{R_e}\nabla^2 \boldsymbol{u}$$

The classical time splitting consists of

1. Convective step

$$\frac{\hat{\boldsymbol{u}} - \boldsymbol{u}^n}{\Delta t} = \boldsymbol{u}^n \times \boldsymbol{\omega}$$

2. Pressure correction step

$$\frac{\hat{\hat{\boldsymbol{u}}} - \hat{\boldsymbol{u}}}{\Delta t} = -\nabla p$$

$$\nabla \cdot \hat{\hat{\boldsymbol{u}}} = 0$$

or

$$\nabla^2 p = \frac{1}{\Delta t} \nabla \cdot (\hat{\hat{\boldsymbol{u}}})$$

3. Viscous step

$$\left(\nabla^2 - \frac{2R_e}{\Delta t}\right)\left(\boldsymbol{u}^{n+1} + u^n\right) = -\frac{2R_e}{\Delta t}\left(\hat{\hat{\boldsymbol{u}}} + \boldsymbol{u}^n\right)$$

Hence in this time splitting, Helmholtz type equations abound, which is why we have been looking at spatially discrete forms of this equation.

2.5 Memory Requirements for SEM

$O(KN^d)$ for iterative method.

$O\left(K^{\frac{2d-1}{d}} N^{2d}\right)$ for direct method.

Direct solvers have been replaced by interative solvers (e.g. preconditioned conjugate gradient method), but may go back again.

2.6 Nonconforming SEM

Define new *Mortar* space that one can project onto and off of at element edges.

Incur more (approximation) errors, but get greater flexibility, particularly in refinement.

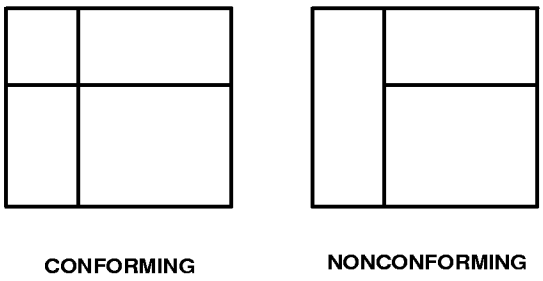

Figure 4: Conforming vs. nonconforming spectral element discretization

2.7 Direct Stiffness Summation

Assembly of the global matrix is required from the elemental matrices. The contributions of the individual elements at common nodes is summed, which in the FEM is termed *direct stiffness summation.*

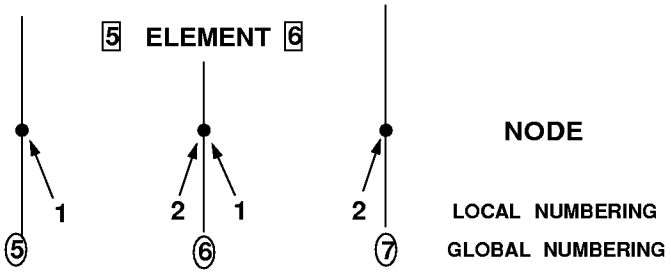

$$u_2^{\boxed{5}} = u_1^{\boxed{6}} = u_{\textcircled{6}}$$

$$A_{ij}^k = \frac{1}{\Delta t}\begin{pmatrix} -1 & 1 \\ 1 & -1 \end{pmatrix}$$

Then direct stiffness sumation imples,

$$A = \frac{1}{\Delta x}\begin{bmatrix} \begin{bmatrix} -1 & 1 \\ 1 & \end{bmatrix} & & & \\ & \begin{bmatrix} -1 & 1 \\ 1 & -1 \end{bmatrix} & & \\ & & \begin{bmatrix} -1 & 1 \\ 1 & -1 \end{bmatrix} & \\ & & & \ddots \end{bmatrix} = \frac{1}{\Delta x}\begin{bmatrix} -1 & 1 & & & \\ 1 & -2 & 1 & & \\ & 1 & -2 & 1 & \\ & & 1 & -2 & 1 \\ & & & & \ddots \end{bmatrix}$$

2.8 Static Condensation of Matrices

The basic strategy is to group nodes according to whether they lie in the boundary or the interior of an element. Since most nodes are in the interior operations involving these nodes do not require any communication accross processors in a parallel environment.

$$\begin{bmatrix} \boldsymbol{A}^k & (\boldsymbol{B}^k)^T \\ \boldsymbol{B}^k & \boldsymbol{C}^k \end{bmatrix} \begin{bmatrix} {}^b\phi^k \\ {}^i\phi^k \end{bmatrix} = \begin{bmatrix} {}^bG^k \\ {}^iG^k \end{bmatrix}$$

On the boundary

$$\sum_k^{\text{DSS}} \left(\boldsymbol{A}^k - (\boldsymbol{B}^k)^T \boldsymbol{C}^k \boldsymbol{B}^k \right) \; {}^b\phi^k = \sum_k^{\text{DSS}} \; {}^bG^k - (\boldsymbol{B}^k)^T (\boldsymbol{C}^k)^{-1} \; {}^iG^k$$

and in the interior

$$\boldsymbol{C}^k \; {}^i\phi^k = \; {}^iG^k - \boldsymbol{B}^k \; {}^b\phi^k$$

The cost estimate for a two dimensional problem is

$O(k^{\frac{3}{2}}N^2)$ for the boundary; and $O(k^2N^4)$ for the interior. As noted the communication overhead for the interior points is absent and hence without communications

$$O\left[(\frac{k}{p})(N^4)\right]$$

3 SPECTRAL-ELEMENT FLUX CORRECTED TRANSPORT METHOD FOR COMPRESSIBLE FLOWS

One deficiency in the Spectral-Element method formulated until fairly recently is that of the limitation of the application to incompressible flows. Spectral methods suffer from their poor representation of discontinuities (Gibbs phenomena in particular, and other phase errors for discontinuities); hence spectral element methods, which use spectral representations locally, inherit these disadvantages. Thus compressible flows have not received much attention, although there have been recent investigations. These new studies have focused, appropriately enough, on flux limiting type algorithms and spectral filtering techniques [11, 29, 12, 2]. Here we describe the spectral element method for compressible flows.

3.1 Application to Hyperbolic Conservation Laws

Consider the conservation law,

$$\frac{\partial w}{\partial t} + \frac{\partial f}{\partial x} = 0,$$

where the vector function w represents density, momentum and total energy, while f is the flux function (giving the 1-D Euler equations). i.e.

$$w = (\rho, \rho V_x, \rho e), \qquad f = (\rho V_x, \rho V_x^2 + p, \rho V_x e + p V_x).$$

Integrating the equation once we obtain the canonical semi-discrete flux form:

$$\frac{\partial w}{\partial t} + \frac{1}{\Delta x}(F_{i+1/2} - F_{i-1/2}) = 0,$$

where it is understood that w is now a *cell-averaged* quantity. The quantity F is an *edge based* quantity derived from the cell-averaged f; this involves a spatial averaging procedure and hence we turn to the spatial discretization.

3.2 Spectral Element Discretization

We will be concerned with cell-averaged quantities and *edge* or *point* quantities. The cell-averaged quantities are defined on the grid j for cell-centered

quantities,

$$x_j, \quad j = 0, N-1 \quad \text{Gauss} - \text{Chebyshev},$$

while the edge quantities are defined over the grid i,

$$x_i = \cos\frac{\pi i}{N} \quad i = 0, N \quad \text{Gauss} - \text{Lobatto} - \text{Chebyshev}.$$

The i grid straddles the j grid as shown in Figure 5. Consider the spatial

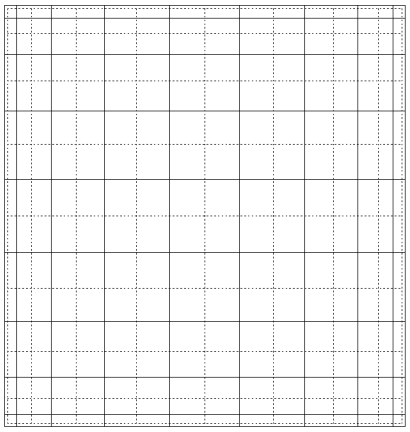

Figure 5: The nodes for the Gauss-Chebyshev points (dashed lines), used for the cell-averaged quantities, and the Gauss-Lobatto-Chebyshev points (solid lines), used for edge quantities, for $N = 9$.

domain partitioned into K elements where in each element, indexed by k,

$$\phi^k(x) = \sum_{i=0}^{N} \phi_i^k h_i(x).$$

Averaging over space gives,

$$\bar{\phi}^k(x) = \sum_{i=0}^{N} \phi_i^k \bar{h}_i(x),$$

where a unique (Lagrange) interpolating function h_i can be found:

$$h_i(x) = \frac{2}{N} \sum_{p=0}^{N} \frac{1}{c_p c_i} T_p(x_i) T_p(x), \quad 0 \le i \le N,$$

and correspondingly,

$$\bar{h}_i(x) = \frac{2}{N} \sum_{p=0}^{N} \frac{1}{c_p c_i} T_p(x_i) \bar{T}_p(x), \quad 0 \le i \le N,$$

with $c_n = 1$ if $n \neq 0, N$ and $c_n = 2$ otherwise. Here,

$$\bar{T}_0 = 1, \quad \bar{T}_1 = \frac{1}{2}\alpha_1 U_1(x), \quad \bar{T}_i = \frac{1}{2}[\alpha_i U_i(x) - \alpha_{i-2} U_{i-2}(x)], \quad i \ge 2,$$

and

$$\alpha_i = \frac{\sin[(i+1)\pi/2N]}{(i+1)\sin(\pi/2N)}.$$

$U_i(x)$ are Chebyshev polynomials of the second kind. The cell-averaging procedure correctly converts point values defined over $N+1$ points to cell-centered average values defined over N points. Note that $h_i(x)$ is an interpolating polynomial, while $\bar{h}_i(x)$ is not.

Analogous to (3.2), there exists a (Lagrange) interpolant taking cell-averaged quantities into a continuous function,

$$\phi^k(x) = \sum_{i=1}^{N} \bar{\phi}_j^k g_j(x).$$

To recover the edge values from the cell-averaged quantities, the following reconstruction is applied:

$$\phi_i = G_j(x_i)\bar{\phi}_j, \quad \text{where} \quad G_j(x) = \sum_{p=0}^{N-1} \frac{\lambda_p^j}{\alpha_p} U_p(x),$$

with

$$\lambda_p^j = \frac{1}{N} T_p(x_j), \quad p = N-2, N-1; \quad \lambda_p^j = \frac{1}{N}[T_p(x_j) - T_{p+2}(x_j)], \quad 0 \le p \le N-3$$

Note that the reconstruction gives only N points, but the interpolating polynomial constructed for the collocation method requires $N+1$ values.

An additional constraint in order to uniquely determine the polynomial is to require C^0 continuity across the interface of the elements so that $\phi_0^{k+1} = \phi_N^k$.

Hence,

$$\phi^{k+1}(\xi) = \sum_{j=1}^{N} \bar{\phi}_j^{k+1} G_j(\xi) + \delta\phi^k,$$

where

$$\delta\phi^k = (1-\xi)T_N'(\xi)\frac{\phi_N^k - \sum_{j=1}^{N} \bar{\phi}_j^{k+1} G_j(-1)}{2N^2}.$$

In (3.2,3.2) we have written (ξ, η, ζ) as the local element coordinate system.

Figure 6a shows the a sinusoid over 32 Gauss points. By use of (3.2) its cell-averaged values $\bar{a}(x)$ are also shown. Figure 6b shows the reconstruction of the function via (3.2,3.2) by plotting the error between the function and its reconstruction. As is evident, the errors are very small.

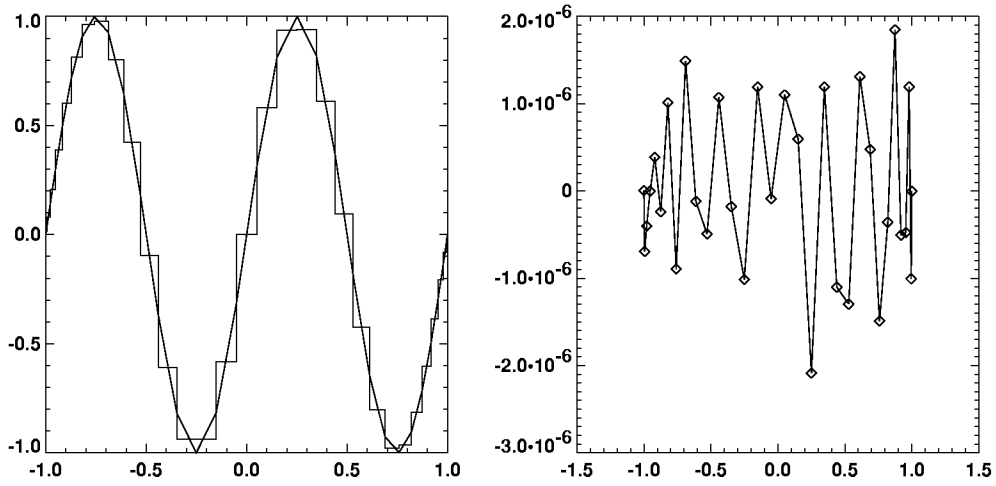

Figure 6: (a) The function $a(x) = \sin 2\pi x$ and its cell average, $\bar{a}(x)$, and (b) The error in the reconstruction from $\bar{a}(x)$ for N=32.

3.3 Flux Corrected Transport

The FCT procedure for solving (3.1) is as follows [1, 35, 36]:

$$\frac{dw}{dt} + \frac{df}{dx} = 0,$$

is

$$w_i^{n+1} = w_i^n - \frac{\Delta t}{\Delta x}(F_{i+1/2} - F_{i-1/2}).$$

The w are interpreted as density, momentum, and the energy; i.e. in 1D $w \equiv \{\rho, \rho u, \rho E\}$ and $f \equiv \{\rho u, \rho u^2 + p, \rho u E + p u\}$. The dependence of F on f is determined by the order of the scheme (see next section). The 3D calculation is extended analogously.

The procedure is as follows,

1. Form a *low-order flux*: $F^L_{i+1/2}$.
2. Form a *high-order flux*: $F^H_{i+1/2}$.
3. Form an *anti-diffusive flux*:
$$A_{i+1/2} = F^H_{i+1/2} - F^L_{i+1/2}.$$
4. Form a *low-order solution*:
$$w_i^L = w_i^n - \frac{\Delta t}{\Delta x}(F^L_{i+1/2} - F^L_{i-1/2}).$$
5. Limit the anti-diffusive flux to prevent spurious extrema in w_i^{n+1}:
$$A^C_{i+1/2} = C_{i+1/2} A_{i+1/2} \qquad 0 \le C_{i+1/2} \le 1.$$
Determination of the appropriate C is the critical and complex step.
6. Update the solution:
$$w_i^{n+1} = w_i^L - \frac{\Delta t}{\Delta x}(A^C_{i+1/2} - A^C_{i-1/2}).$$

In the Spectral Element-FCT approach we define the cell-centered quantities to be on the Gauss-Chebyshev points (grid j) while the fluxes are on the Gauss-Lobatto-Chebyshev points (grid i). Step 2 above is interpreted in the Spectral Element formulation. Fluxes are obtained via (3.2,3.2) from the cell-centered flux function as in (3.1).

3.4 Shock Tube Results

We solve a one-dimensional hydrodynamics problem — the shock tube — with parameters due to Sod [30]. At time $t = 0$ the gas on the left of a diaphragm is at pressure $p = 1, \rho = 0.1$ while on the right it is at $p = 1, \rho = 0.125$. Following the rupture of the diaphragm at $t = 0^+$, three waves propagate through the gas: an expansion fan, a contact discontinuity and a shock wave. Figure 7 shows the results obtained with the spectral-element FCT method with $N = 21, K = 20$. While not exceptional, the method does quite well. Some small excrescences are evident.

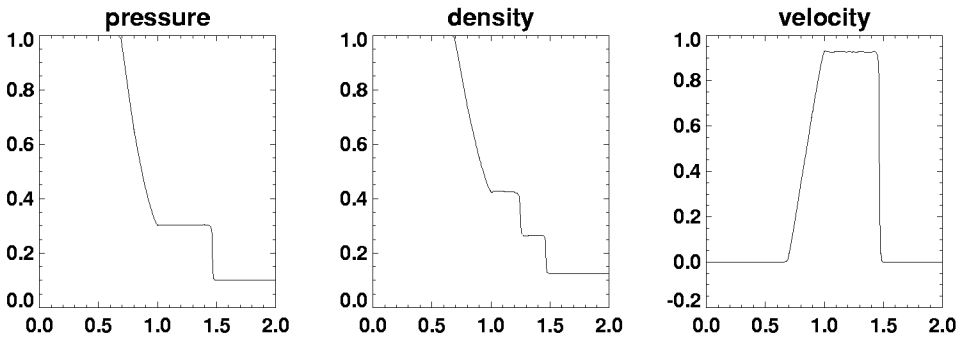

Figure 7: Shock tube results. Time is 0.263, $N = 21$, $K = 20$. Parameter are those due to Sod.

4 STABILITY OF NUMERICAL SCHEMES

4.1 Von Neumann Stability Analysis

In so-called "α" - methods for solving

$$\frac{\partial u}{\partial t} = f(u) = \nu \frac{\partial^2 u}{\partial x^2} \tag{13}$$

The discretization of time leads to

$$\frac{u^{n+1} - u^n}{\Delta t} = \nu \left[\alpha f(u^{n+1}) + (1-\alpha) f(u^n) \right]$$

$$= \nu \left[\alpha u_{xx}^{n+1} + (1-\alpha) u_{xx}^n \right]$$

Here if

$\alpha = 0$ Forward Euler — 1st order explicit
$\alpha = \frac{1}{2}$ Crank-Nicolson 2nd order implicit
$\alpha = 1$ Backward Euler — 1st order implicit

For instance,

$$\frac{u^{n+1} - u^n}{\Delta t} = \nu\alpha \left(\frac{u_{i+1}^{n+1} - 2u_i^{n+1} + u_{i-1}^{n+1}}{\Delta x^2} \right) + \nu(1-\alpha) \left(\frac{u_{i+1}^n - 2u_i^n + u_{i-1}^n}{\Delta x^2} \right)$$

Since the problem is linear, use single mode

$$u \propto a_k e^{ikx}$$

$$u_{xx} = -a_k k^2 e^{ikx}$$

Applying

$$e^{ikx}\left\{a_k^{n+1} - a_k^n = r\left[-\alpha k^2 a_k^{n+1} - (1-\alpha)k^2 a_k^n\right]\right\}$$

where

$$r = \nu\frac{\Delta t}{\Delta x^2}$$

or

$$a_k^{n+1} = a_k^n\left[\frac{1 - r(1-\alpha)k^2}{1 + r\alpha k^2}\right]$$

For $\alpha = 0$ Forward Euler

$$\alpha_k^{n+1} = a_k^n\left(1 - rk^2)\right)$$

Stability requires

$$|1 - rk^2| \leq 1$$

or

$$-1 \leq \nu\frac{\Delta t}{\Delta x^2}k^2 \leq 1$$

or

$$\frac{\Delta t}{\Delta x} \leq \frac{\Delta x}{\nu k^2}$$

$$\sigma \leq \frac{\Delta x}{\nu k^2}$$

σ is the *Courant number*.

For fixed σ, Δx, ν, Large enough k will always violate the condition. High wave numbers or, equivalently, short wavelengths will always be unstable. Thus forward Euler is always unstable for a diffusion type equation. Note that the stability properties of a numerical scheme depend not only on the scheme but also on the particular differential equation being considered.

For $\alpha = 1$ Backwards Euler

$$\alpha_k^{n+1} = a_k^n \left(\frac{1}{1 + rk^2} \right)$$

Stability requires

$$\left| \frac{1}{1 + rk^2} \right| \leq 1$$

which is true for all k, and therefore the method is stable.

For $\alpha = \frac{1}{2}$ Crank-Nicolson

$$\alpha_k^{n+1} = a_k^n \left(\frac{1 - \frac{1}{2} rk^2}{1 + \frac{1}{2} rk^2} \right)$$

Stability requires

$$\left| \frac{2 - rk^2}{2 + rk^2} \right| \leq 1$$

or

$$2 - rk^2 \leq 2 + rk^2$$

be true for all k. Indeed this condition is satisfied for all k. However for very large k the amplification, $\frac{\alpha_k^{n+1}}{a_k^n} \to -1$; similarly for fixed k and $\sigma \uparrow$, the amplifications tends to -1.

We note that we have used

$$u_{xx} = -k^2 u$$

Which assumes we have a spectral (Fourier) respresentation of the spatial operator. For finite differences other cofficients will occur and for other operators complex coefficients can occur.

5 READING GUIDE

Introductory Reading

- Of course, *The* introduction to any numerical work — [26].

Spectral Methods Ingredients

- Fast Fourier Transforms — [33, 34].
- Numerical Integration — [19], [6].
- Chebyshev polynomials — [27].
- General (non-spectral method specific) stability analysis — [17].
- Direct and Iterative solvers — [13].

Spectral Methods for PDEs

- New book on pseudospectral methods — [10].
- *The* books on spectral methods — [14, 3].
- Boundary Layers — [31].
- Poisseulle flow — [23].
- Channel flow — [22].
- Rayleigh-Benard Convection — [4, 16].
- Double-Diffusive Convection (only the Poisson eqn. solved spectrally) — [18, 7].
- Spectral methods application to MHD — [24, 5].
- Taylor-Couette Flow — [32].
- Mixing Layers — [21].

Spectral-Element Methods for PDEs

- Original paper on Spectral-Elements — [25].
- Legendre Spectral-Elements —[28].
- Parallel Spectral-Elements — [9, 8].

- Non-conforming Spectral-Elements — [20]
- Spectral-Elements and Finite-Difference Hybrid schemes — [15].

References

[1] J. P. Boris and D. L. Book. Flux Corrected Transport I: SHASTA a fluid transport algorithm that works. *J. Comput. Phys.*, 11:38–69, 1973.

[2] W. Cai, D. Gottlieb, and A. Harten. Cell averaging Chebyshev methods for hyperbolic problems. Technical Report 90-27, ICASE, NASA Langley Research Center, 1990.

[3] C. Canuto, M. Y. Hussaini, A. Quarteroni, and T. A. Zang. *Spectral Methods in Fluid Dynamics.* Springer-Verlag, 1988.

[4] J. H. Curry, J. R. Herring, S. A. Orszag, and J. Loncaric. Order and disorder in two and three dimensional Benard convection. *J. Fluid Mech.*, 147:1–38, 1984.

[5] R. B. Dahlburg and J. M. Picone. Evolution of the Orszag-Tang vortex system in a compressible medium. I. initial average subsonic flow. *Phys. Fluids B*, 1:2153–2171, 1989.

[6] P.J. Davis and P. Rabinowitz. *Methods of Numerical Integration.* Academic Press, 1975.

[7] A. E. Deane, E. Knobloch, and J. Toomre. Traveling waves and chaos in thermosolutal convection. *Phys. Rev. A*, 36(6):2862–2869, 1987.

[8] P. Fischer, E. M. Ronquest, and A. T. Patera. Parallel spectral-element methods for viscous flow. In G. F. Carey, editor, *Parallel Supercomputing Methods, Algorithms and Applications*, pages 223–232. Chichester, Wiley, 1989.

[9] P. F. Fischer and A. T. Patera. Parallel spectral element solution of the Stokes problem. *to appear in J. Comput. Phys.*, 1990.

[10] B. Fornberg. *A Practical Guide to Psuedospectral Methods.* Cambridge, 1996.

[11] J. Giannakouros and G.E. Karniadakis. Spectral element-FCT method for scalar hyperbolic conservation laws. *Int. J. Num. Meth. Fluids*, 14:707–727, 1992.

[12] J. Giannakouros and G.E. Karniadakis. A Spectral Element-FCT method for the compressible Euler equations. *J. Comput. Phys.*, 115:65–85, 1994.

[13] G. H. Golub and C. F. Van Loan. *Matrix Computations.* Johns Hopkins University Press, 1989.

[14] D. Gottleib and S.A. Orszag. *Numerical Analysis of Spectral Methods: Theory and Applications.* SIAM-CBMS, 1977.

[15] R. Henderson and G. E. Karniadakis. Hybrid spectral-element-low-order methods for incompressible flows. *J. Scientific Comput.*, 6(2):79–100, 1991.

[16] J. R. Herring and J. C. Wyngaard. Convection with a simple chemically reactive passive scalar. In *5th Symp. on Turb. Shear Flows*, pages 10.39–10.43, 1985.

[17] C. Hirsch. *Numerical Computation of Internal and External Flows, Volumes 1&2.* Wiley, 1988.

[18] E. Knobloch, D. R. Moore, J. Toomre, and N. O. Weiss. Transitions to chaos in two-dimensional double-diffusive convection. *J. Fluid Mech.*, 166:409–448, 1986.

[19] V. I. Krylov. *Approximate Calculation of Integrals.* Macmillan, 1962.

[20] C. A. Mavriplis. *Nonconforming Discretizations and a Posteriori Error Estimators for Adaptive Spectral Element Techniques.* PhD thesis, M.I.T., Cambridge, MA., 1989.

[21] R. W. Metcalf, S. A. Orszag, M. E. Brachet, S. Menon, and J. Riley. Secondary instability of a temporally growing mixing layer. *J. Fluid Mech.*, 184:207–243, 1987.

[22] P. Moin and J. Kim. Numerical investigation of turbulent channel flow. *J. Fluid Mech.*, 118:341–377, 1982.

[23] S. A. Orszag and L. C. Kells. Transition to turbulence in plane Poiseuille flow and plane Couette flow. *J. Fluid Mech.*, 96:159–205, 1980.

[24] S. A. Orszag and C. M. Tang. Small-scale structure of two-dimensional magnetohydrodynamic turbulence. *J. Fluid Mech.*, 90:129–143, 1979.

[25] A. T. Patera. A spectral element method for fluid dynamics: Laminar flow in a channel expansion. *J. Comput. Phys.*, 54:468–488, 1984.

[26] W. H. Press, B. P. Flannery, S. A. Teukolsky, and W. T. Vetterling. *Numerical Recipes.* Cambridge University Press, 1986.

[27] T. J. Rivlin. *The Chebyshev Polynomials.* Wiley Interscience, 1974.

[28] E.M. Ronquist and A.T. Patera. A Legendre spectral-element method for the incompressible Navier-Stokes equations. In *Proc. 7th GAMM Conf. Numerical Methods in Fluid Mechanics*, pages 318–326. Vieweg,Braunschweig, 1988.

[29] D. Sidilkover and G. E. Karniadakis. Non-oscillatory spectral element Chebyshev method for shock wave calculations. *J. Comput. Phys.*, 107:10–22, 1993.

[30] G.A. Sod. A survey of several finite difference methods for systems of nonlinear hyperbolic conservation laws. *J. Comput. Phys.*, 27:1–31, 1978.

[31] P. R. Spalart. Numerical simulations of boundary layers, Part1: Weak formulation and numerical method. Technical report, NASA TM-88222, 1986.

[32] C. L. Streett and M. Y. Hussaini. Finite length Taylor-Couette flow. In D.L. Dwoyer and M.Y. Hussaini, editors, *The Stability of Time-dependent/Spatially Varying Flows*, pages 312–334. Springer-Verlag, 1987.

[33] C. Temperton. A new set of minimum-add small-n rotated DFT modules. *J. Comput. Phys.*, 75:190–198, 1988.

[34] C. Temperton. A self-sorting in-place prime factor real/half-complex FFT algorithm. *J. Comput. Phys.*, 75:199–216, 1988.

[35] S. Zalesak. Fully multidimensional Flux Corrected Transport algorithms for fluids. *J. Comput. Phys.*, 31(3):335–362, 1979.

[36] S. Zalesak. High order zip differencing of convective terms. *J. Comput. Phys.*, 40(2):497–508, 1981.

REPORT DOCUMENTATION PAGE

Form Approved
OMB No. 0704-0188

1. AGENCY USE ONLY *(Leave blank)*	2. REPORT DATE	3. REPORT TYPE AND DATES COVERED
	June 1997	Contractor Report

4. TITLE AND SUBTITLE
Spectral and Spectral–Element Methods: Lecture Notes in High Performance Computational Physics

5. FUNDING NUMBERS
Code 931

6. AUTHOR(S)
Anil E. Deane

7. PERFORMING ORGANIZATION NAME(S) AND ADDRESS (ES)
George Mason University
Fairfax, VA 22030-4444

8. PEFORMING ORGANIZATION REPORT NUMBER
97B00056

9. SPONSORING / MONITORING AGENCY NAME(S) AND ADDRESS (ES)
National Aeronautics and Space Administration
Washington, DC 20546-0001

10. SPONSORING / MONITORING AGENCY REPORT NUMBER
CR–203877

11. SUPPLEMENTARY NOTES
Anil Deane: George Mason University, Fairfax, VA 22030-4444

12a. DISTRIBUTION / AVAILABILITY STATEMENT
Unclassified - Unlimited
Subject Category: 75
This report is available from the NASA Center for AeroSpace Information, 800 Elkridge Landing Road, Linthicum Heights, MD 21090;301-621-0390

12b. DISTRIBUTION CODE

13. ABSTRACT *(Maximum 200 words)*

This is an introduction to spectral and spectral–element methods for the numerical simulation of incompressible and compressible hydrodynamics. The theory behind the methods is presented as well as some examples of working codes. The work is reasonably self-contained in that there is included a discussion of numerical quandrature, weighted residual methods, Fast Fourier Transforms, and time marching schemes. The work is based on a set of lectures by the author for the NASA Summer School for High Performance Computational Physics, held at the Goddard Space Flight Center.

14. SUBJECT TERMS
Spectral Methods; Spectral–element Methods; Lecture Notes

15. NUMBER OF PAGES
62

16. PRICE CODE

17. SECURITY CLASSIFICATION OF REPORT	18. SECURITY CLASSIFICATION OF THIS PAGE	19. SECURITY CLASSIFICATION OF ABSTRACT	20. LIMITATION OF ABSTRACT
Unclassified	Unclassified	Unclassified	UL